

# UC Davis

## UC Davis Previously Published Works

### Title

Efficacy of Combined Histone Deacetylase and Checkpoint Kinase Inhibition in a Preclinical Model of Human Burkitt Lymphoma

### Permalink

<https://escholarship.org/uc/item/6p9610z1>

### Journal

Molecular Medicine, 21(1)

### ISSN

1076-1551

### Authors

Kong, YanGuo  
Barisone, Gustavo A  
Sidhu, Ranjit S  
[et al.](#)

### Publication Date

2015

### DOI

10.2119/molmed.2015.00032

Peer reviewed

# Efficacy of Combined Histone Deacetylase and Checkpoint Kinase Inhibition in a Preclinical Model of Human Burkitt Lymphoma

YanGuo Kong,<sup>1,2,\*</sup> Gustavo A Barisone,<sup>1,\*</sup> Ranjit S Sidhu,<sup>1</sup> Robert T O'Donnell,<sup>1,3</sup> and Joseph M Tuscano<sup>1,3</sup>

<sup>1</sup>Division of Hematology and Oncology, Department of Internal Medicine, University of California Davis School of Medicine, Sacramento, California, United States of America; <sup>2</sup>Department of Neurosurgery, Peking University Medical College Hospital, Chinese Academy of Medical Sciences, Beijing, China; and <sup>3</sup>Department of Veterans Affairs, Northern California Healthcare System, Sacramento, California, United States of America

Checkpoint kinase inhibition has been studied as a way of enhancing the effectiveness of DNA-damaging agents. More recently, histone deacetylase inhibitors have shown efficacy in several cancers, including non-Hodgkin lymphoma. To evaluate the effectiveness of this combination for the treatment of lymphoma, we examined the combination of AR42, a histone deacetylase inhibitor, and checkpoint kinase 2 (CHEK2) inhibitor II *in vitro* and *in vivo*. The combination resulted in up to 10-fold increase in potency in five Burkitt lymphoma cell lines when compared with either drug alone. Both drugs inhibited tumor progression in xenograft models, but the combination was more effective than either agent alone, resulting in regression of established tumors. No toxicity was observed. These results suggest that the combination of histone deacetylase inhibition and checkpoint kinase inhibition represent an effective and nontoxic treatment option that should be further explored in preclinical and clinical studies.

**Online address:** <http://www.molmed.org>

**doi:** 10.2119/molmed.2015.00032

## INTRODUCTION

Non-Hodgkin lymphoma (NHL) is the sixth most common cause of cancer-related death in the United States and its incidence has nearly doubled since the early 1970s. Over 65,000 new cases of NHL are diagnosed each year in the United States and approximately 332,000 people are currently living with this disease (1–3). While current treatments have resulted in improved response rates, the majority of patients with NHL still succumb to this disease. The toxicity of current therapy often limits its efficacy, especially in the elderly.

The use of epigenetic modulators has had some success in the treatment of a number of malignancies, including NHL. Histone deacetylases mediate chromatin remodeling by removing acetyl groups from lysine residues in the core histones, which results in a more compact, transcriptionally repressed chromatin. Histone deacetylase inhibitors (HDACIs) have been shown to inhibit the proliferation of cancer cells *in vitro* and *in vivo* in a variety of malignancies (4–9), including lymphoma (10–14). HDACIs are hypothesized to suppress cancer cell proliferation through histone hyperacetylation, resulting

in more relaxed chromatin, making it more accessible to DNA-damaging agents and changing the expression of genes involved in DNA damage recognition and repair, apoptosis and tumor suppression (15). Besides their effect on chromatin remodeling, over 50 transcription factors, DNA repair enzymes and other proteins have been shown to be targets of HDACIs (16). Currently, three such drugs are FDA-approved for the treatment of NHL (vorinostat, belinostat and romidepsin); a number of others are in clinical development for various hematologic malignancies (17,18). AR42, a phenylbutyrate-derived pan-HDACI, has been shown to have cytotoxic activity in several malignancies (4–7,9,19,20). More recently, AR42 and other HDACIs have been reported to synergistically increase the cytotoxic activity of the  $\alpha$ -CD22 monoclonal antibody (mAb) HB22.7 (14) and the  $\alpha$ -CD20 mAb rituximab (11–13) on NHL cells.

Checkpoint kinases 1 and 2 (CHEK1 and CHEK2) are part of the DNA damage recognition and repair cascade; their activation leads to cell cycle

\*YK and GAB contributed equally to this work.

**Address correspondence to** Joseph M Tuscano, Department of Internal Medicine, Division of Hematology and Oncology, University of California Davis Health System, 4501 X Street, Suite 3016, Sacramento, CA 95817. Phone: 916-734-3771; Fax: 916-734-7946; E-mail: [joseph.tuscano@ucdmc.ucdavis.edu](mailto:joseph.tuscano@ucdmc.ucdavis.edu).

Submitted February 11, 2015; Accepted for publication August 20, 2015; Published Online ([www.molmed.org](http://www.molmed.org)) August 24, 2015.

The Feinstein Institute  
for Medical Research 

Empowering Imagination. Pioneering Discovery.®

arrest, allowing for DNA repair to occur. Inhibitors of CHEK1 and CHEK2 abrogate the physiological cell cycle arrest induced by DNA damage, thereby preventing repair and allowing the propagation of chromosomal aberrations. CHEK2 phosphorylates a range of proteins involved in cell cycle control and apoptosis, including cdc25A, cdc25C, Mdmx, p53, BRCA1, PML, E2F1 and phosphatase 2A (21). Cells derived from CHEK2-deficient mice exhibit defects in their ability to delay entry into S phase, sustain a G2 cell cycle arrest and undergo apoptosis in response to DNA damage (22). CHEK2 is required for proper progression of mitosis and for the maintenance of chromosomal stability, independent of p53 and DNA damage (23). CHEK2 can also protect genome integrity by promoting apoptosis through interacting with a number of other substrates. Inhibition of CHEK2 by transfection of a dominant-negative CHEK2 mutant or a chemical inhibitor, debromohymenialdesine, stabilizes centrosomes, maintains high cyclin B1 levels and allows for a prolonged activation of Cdk1 (24). Under these conditions, multinuclear HeLa syncytia do not arrest at the G2/M boundary and rather enter mitosis and subsequently die during metaphase (24). Therefore, inhibition of CHEK2 can sensitize proliferating cells to chemotherapy-induced apoptosis. Targeting of CHEK2 with small interfering RNA prevents survivin release from the mitochondria and enhanced apoptosis following induction of DNA damage by ionizing radiation or doxorubicin and inhibits the growth of resistant tumors *in vivo*. Expression of a dominant negative CHEK2 potentiates cytotoxicity in HCT116 colon carcinoma cells to doxorubicin (25). CHEK2 inhibitors have been shown to be effective against myc-driven NHL, where inhibition of CHEK kinases results in marked enhancement of DNA damage and apoptosis (26).

Here, we examine the effects of combining the HDACi AR42 and the CHEK2 inhibitor II (CHEK2i) on *in vitro* cytotoxicity and *in vivo* efficacy using human NHL

cell lines and a human NHL xenograft model. This report is the first to examine the effects of these two agents on human NHL cells. These studies show that this combination has synergistic *in vitro* and *in vivo* lymphomacidal activity and, given the availability of FDA-approved HDACis, this represents a promising strategy for human clinical trials.

## MATERIALS AND METHODS

### Reagents

AR42 (OSU-HDAC42, (S)-N-hydroxy-4-(3-methyl-2-phenylbutanamido)benzamide) was purchased from Selleckchem. The CHEK2 inhibitor II (CHEK2i) 2-(4-(4-chlorophenoxy)phenyl)-1H-benzimidazole-5-carboxamide hydrate was obtained from Sigma-Aldrich. Goat anti-mouse IgG PE-Cy5 was purchased from Santa Cruz Biotechnology. Anti-p21 and  $\beta$ -actin antibodies were purchased from Cell Signaling Technology. MTS-based cell proliferation kits and secondary antibodies conjugated to HRP were purchased from Promega.

### Cell Lines

The lymphoma cell lines CA46, Raji, Ramos, Daudi, DG75 and HAMALWA were purchased from American Type Culture Collection (ATCC). All cells were grown in RPMI-1640 medium supplemented with 10% fetal bovine serum (FBS), 100 U/mL penicillin G and 100  $\mu$ g/mL streptomycin and incubated at 37°C in a humidified 5% CO<sub>2</sub> incubator.

### In Vitro Cytotoxicity

Cells were plated in 96-well plates at a density of  $5 \times 10^4$  cells/well in 100  $\mu$ L media and treated with CHEK2i (20 to 0.15  $\mu$ mol/L), AR42 (2 to 0.03  $\mu$ mol/L) or a combination of AR42 (0.03 to 2.00  $\mu$ mol/L in two-fold increments) with a fixed dose of CHEK2i (5  $\mu$ mol/L). After up to 72 h of incubation, cell viability was assessed using the CellTiter 96 Aqueous One Solution Cell Proliferation Assay (Promega) according to the manufacturer's instructions. Cell viability as a percent of the untreated control

was calculated as follows:  $([\text{OD}_{490} \text{ treated} - \text{OD}_{490} \text{ background}] / [\text{OD}_{490} \text{ control} - \text{OD}_{490} \text{ background}]) * 100$ . The mean  $\pm$  standard deviation (SD) of three separate experiments performed in triplicate is shown.

### Cell Cycle

Cell cycle subpopulations were quantified by DNA content measured by flow cytometry after propidium iodide (PI) staining. Cells ( $10^6$ ) were collected after treatment by centrifugation for 5 min at 200g, washed twice with cold PBS, resuspended in 0.5 mL of PBS and fixed overnight in ice-cold 70% ethanol at -20°C. For PI staining, the cells were washed with cold PBS and resuspended in 1 mL of 20 mg/mL PI, 0.1% Triton X-100 and 200 mg/mL RNase A in PBS for 30 min at RT. Data was acquired using a Becton Dickinson FACSCalibur cytometer and fitted with FlowJo software (Tree Star Inc.) using the Watson Pragmatic model.

### Apoptosis

Cells ( $1 \times 10^6$ /mL) were incubated with AR42 (1  $\mu$ mol/L), CHEK2i (5  $\mu$ mol/L) or both for 24 or 72 h, washed in cold PBS and resuspended in annexin binding buffer (10 mmol/L HEPES, 140 mmol/L NaCl, 2.5 mmol/L CaCl<sub>2</sub>, pH 7.4). One hundred  $\mu$ L of the cell suspension were stained with 5  $\mu$ L of annexin-FITC (BD Pharmingen) and 1  $\mu$ g/mL PI according to the manufacturer's instructions. Data (50,000 events/sample) were acquired in a Becton Dickinson FACSCanto instrument and analyzed with FlowJo software. Untreated cells were stained as controls. Unstained and single-stain controls were used for compensation.

### Clonogenic Survival Assay

Colony formation assays in soft agar were performed as described previously (14). Cells were treated for 7 d with 1.6  $\mu$ mol/L CHEK2i, 0.25  $\mu$ mol/L AR42 or the combination of both. Controls were treated with vehicle only. The colonies that formed from surviving cells were fixed with a mixture of methanol and acetic acid (10:1, v/v) and stained

with 1% crystal violet in methanol. Colonies >5 mm were counted and the fraction of surviving cells was calculated.

### Immunoblot Analysis

Raji cells ( $10^7$  cells) were treated with 1  $\mu\text{mol/L}$  AR42 and/or 5  $\mu\text{mol/L}$  CHEK2i for 24 h and collected by centrifugation, washed with PBS, and suspended in lysis buffer (20 mmol/L Tris-HCl pH 7.4, 150 mmol/L NaCl, 1 mmol/L EDTA, 1 mmol/L EGTA, 1% Triton X-100, 1 mmol/L  $\text{Na}_3\text{VO}_4$ , 1 mg/mL aprotinin, 1 mg/mL leupeptin and 1 mmol/L PMSF). Equal amounts of protein lysate were separated by SDS-PAGE, and transferred to PVDF membrane (Millipore). The membranes were probed with primary antibodies for p21 and  $\beta$ -actin (as a load control) overnight at 4°C followed by secondary antibodies conjugated to HRP and visualized by enhanced chemiluminescence (ECL).

### Xenograft Studies

Female, 6–8-wk-old female athymic nude mice (Harlan) were maintained in microisolation cages under pathogen-free conditions in the University of California–Davis animal facility. All procedures were conducted under an approved protocol according to guidelines specified by the National Institutes of Health–adopted *Guide for the Care and Use of Laboratory Animals* (eighth edition, 2011). Mice were allowed to acclimatize for at least 4 d

prior to the start of any experiment. Three days after whole body irradiation (400 rads),  $5 \times 10^6$  Raji cells in 100  $\mu\text{L}$  PBS were implanted subcutaneously in the flank to establish tumors. After tumors reached  $>300 \text{ mm}^3$ , mice were randomly assigned to one of four treatment groups (7 animals/group): control (vehicle only), CHEK2i (1.0 mg/kg/dose), AR42 (10 mg/kg/dose), or combination of CHEK2i (1.0 mg/kg/dose) and AR42 (1.0 mg/kg/dose). Doses were based on previously published studies (14,27). Treatment consisted of intraperitoneal injections every other day for 45 d. Tumor size was measured three times per week and volume was calculated as  $d_1 \times d_2 \times d_3 \times 0.52$ . Blood was collected at the indicated times for toxicity analysis and body weight was recorded for the length of the study.

### Statistical Analysis

*In vitro* cytotoxicity data, soft agar colony formation assays and resected tumor weight were analyzed by a two-tailed, unpaired Student *t* test. To obtain  $\text{IC}_{50}$  values, the dose-response data was fitted to a dose-response-inhibition curve. All statistical analysis was performed using GraphPad Prism software. A *p* value of  $<0.05$  was considered significant. For pharmacological interactions, additive versus synergistic effects of the drugs were evaluated using CompuSyn software (28).

## RESULTS

### Cytotoxic Effects of AR42 and CHEK2i on NHL Cell Lines

The cytotoxicity of AR42 and CHEK2 inhibitor II both individually and in combination was initially examined in Raji NHL cells. Cells were treated at indicated concentrations and assessed using a viability assay at 12, 36 and 72 h. Consistent with previous studies, both agents were cytotoxic when used alone, with statistically significant differences (relative to untreated controls) observed at 36 and 72 h. Treatment with the combination of AR42 and CHEK2i resulted in increased cell death. Indeed, significantly higher cytotoxicity was observed with the combination as early as 12 h after treatment when compared with either drug alone, and this continued over a 72-h time course (Figure 1A). To further evaluate the cytotoxic potential of the inhibitor combination, we extended the analysis by determining the  $\text{IC}_{50}$  of either drug alone and the combination on 5 NHL cell lines: CA46, DG75, NAMALWA, Raji and Ramos. All the cell lines were similarly sensitive to AR42 (Figure 1B, left panel), while CHEK2i was more cytotoxic for Raji and Ramos (Figure 1B, center panel). The cytotoxicity of the combination was examined by dose-escalating AR42 combined with a fixed dose of CHEK2i (5  $\mu\text{mol/L}$ ). The combination

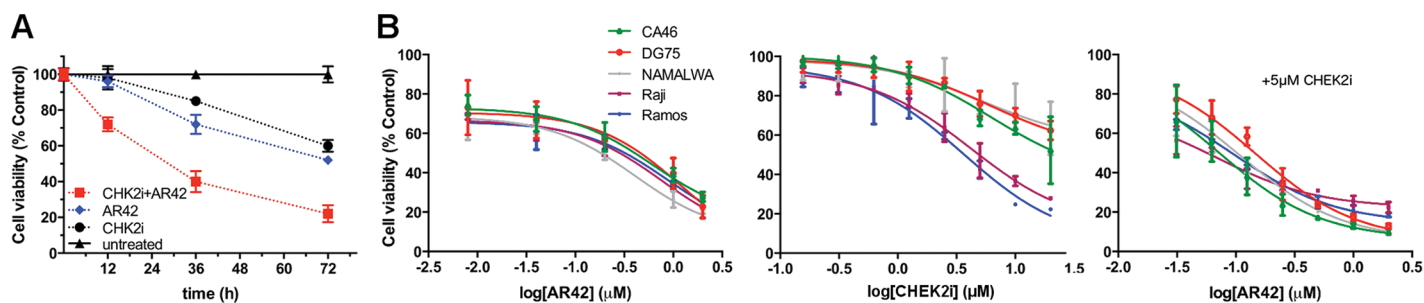


**Figure 1.** *In vitro* cytotoxicity of AR42 and CHEK2 inhibitor against NHL cell lines. (A) Treatment of Raji cells with AR42 (1  $\mu\text{mol/L}$ ) and CHEK2i (5  $\mu\text{mol/L}$ ) resulted in decreased viability when compared with untreated controls. The combination of both inhibitors resulted in greater and earlier cell death when compared with either drug alone. (B) Dose-response curves for AR42 (left), CHEK2i inhibitor (center) and the dose escalation of AR42 combined with a fixed dose of CHEK2i (5  $\mu\text{mol/L}$ ) (right) show enhanced cytotoxicity of the combination. Cell viability was measured using an MTS assay and the mean of three separate experiments performed in triplicate.

**Table 1.** IC<sub>50</sub> values (with 95% confidence interval) for AR42, CHEK2i and AR42 combined with CHEK2i (5 μmol/L) on NHL cell lines.

NHL cells	IC <sub>50</sub> (95% CI)		
	AR42 (μmol/L)	CHEK2i (μmol/L)	AR42 (μmol/L) + CHEK2i
CA46	0.61 (0.36–1.03)	6.30 (4.16–9.56)	0.07 (0.05–0.11)
DG75	1.21 (0.46–3.17)	6.06 (4.18–8.80)	0.15 (0.10–0.21)
NAMALWA	0.41 (0.29–0.57)	5.27 (2.56–10.81)	0.11 (0.08–0.15)
Raji	0.75 (0.46–1.23)	4.20 (3.34–5.29)	0.07 (0.04–0.12)
Ramos	0.87 (0.50–1.51)	3.64 (2.70–4.89)	0.10 (0.07–0.14)

of both inhibitors was more cytotoxic than either drug alone (Figure 1B, right panel). The IC<sub>50</sub> ranged from 0.4 μmol/L (NAMALWA) to 1.2 μmol/L (DG75) for AR42 and from 3.6 μmol/L (Ramos) to 6.3 μmol/L (CA46) for CHEK2i, while the IC<sub>50</sub> for the combination were between 0.07 and 0.15 μmol/L, representing a four-fold (NAMALWA) to 10-fold (Raji) increase in potency (Table 1). This increase was achieved with a fixed dose of CHEK2i of 5 μmol/L, which is near its IC<sub>50</sub> for the cell lines used in this study. The combined effect of AR42 and CHEK2i was synergistic, as determined by isobologram analysis and combination index (CI). CI values <1, (indicative of synergism, 29) were obtained in all five cell lines (Table 2).

### CHEK2i Enhances AR42 Inhibition of Cell Cycle Progression

Since both histone deacetylase inhibition and checkpoint kinase inhibition are known to modulate the cell cycle, we evaluated the effects of AR42, CHEK2i and the combination on cell

cycle progression in Raji cells. When compared with untreated controls, treatment with AR42 resulted in an increase in the G0/G1 population, suggesting a G1 arrest (Figures 2A, B). On the other hand, treatment with CHEK2i increased the S population, consistent with abrogation of the G1/S checkpoint as expected (Figures 2A, B). Treatment with the combination of both inhibitors resulted in a further increase in the G0/G1 population when compared with either untreated controls or single drug treatments; the S phase was reduced when compared with CHEK2i alone, as was the G2/M population when compared with all other groups. In all cases, the magnitude of change in cell cycle phases was small but statistically significant ( $p < 0.05$ ) when analyzed by two-way ANOVA with Tukey multiple comparison test (Table 3).

To determine if the observed changes in cell cycle correlated with expression of the cell cycle regulators p21 and/or TP53, Raji cells were examined for p21 expression using immunoblotting. Treatment with CHEK2i resulted in

a mild increase in p21 levels, while AR42 treatment markedly increased the protein level (Figure 2C). The combination treatment did not seem to further increase p21 levels beyond those induced by AR42 alone. TP53 levels were not affected by any of the treatments, nor was its activity, as assessed by the levels of phosphorylated TP53 protein (Figure 2C).

### AR42, but Not CHEK2i, Induced Apoptosis in NHL Cells

To further investigate the mechanisms by which these drugs exert lymphomacidal activity, we stained cells for early apoptosis using annexin V. Counterstaining with PI was used to identify late-apoptotic and necrotic cells. As shown in Figure 2D, and consistent with what has been reported previously (10), a substantial increase in the apoptotic population was observed when CA46 cells were treated with AR42. Treatment with CHEK2i, however, did not result in increased apoptosis when compared with untreated controls, even after 72 h of incubation. When used in combination with AR42, CHEK2i did not further increase the apoptotic effect of AR42. Similar results were obtained for all cell lines in this study (Figure 2E). When compared with untreated controls, there was a significant ( $p < 0.01$ ) increase in apoptosis after treatment with AR42 or the combination, but not after treatment with CHEK2i alone. The apoptotic effect of the combination was not significantly different from that of AR42 alone.

**Table 2.** Combination index of AR42 and CHEK2i.

AR42 (μmol/L)	CHK2i (μmol/L)	DG75		NAMALWA		Raji		Ramos		CA46	
		Effect	CI	Effect	CI	Effect	CI	Effect	CI	Effect	CI
2	5	0.128	0.071	0.099	0.085	0.224	0.569	0.186	0.129	0.902	0.023
1	5	0.174	0.106	0.151	0.148	0.258	0.574	0.208	0.110	0.870	0.034
0.5	5	0.239	0.170	0.202	0.184	0.310	0.707	0.250	0.134	0.828	0.051
0.25	5	0.342	0.346	0.324	0.479	0.333	0.634	0.324	0.255	0.763	0.086
0.125	5	0.583	2.224	0.436	0.823	0.371	0.686	0.429	0.661	0.618	0.257
0.0625	5	0.681	3.748	0.635	3.348	0.515	1.791	0.621	4.881	0.441	0.968
0.03125	5	0.772	6.94	0.712	4.153	0.564	2.089	0.645	4.829	0.337	1.956

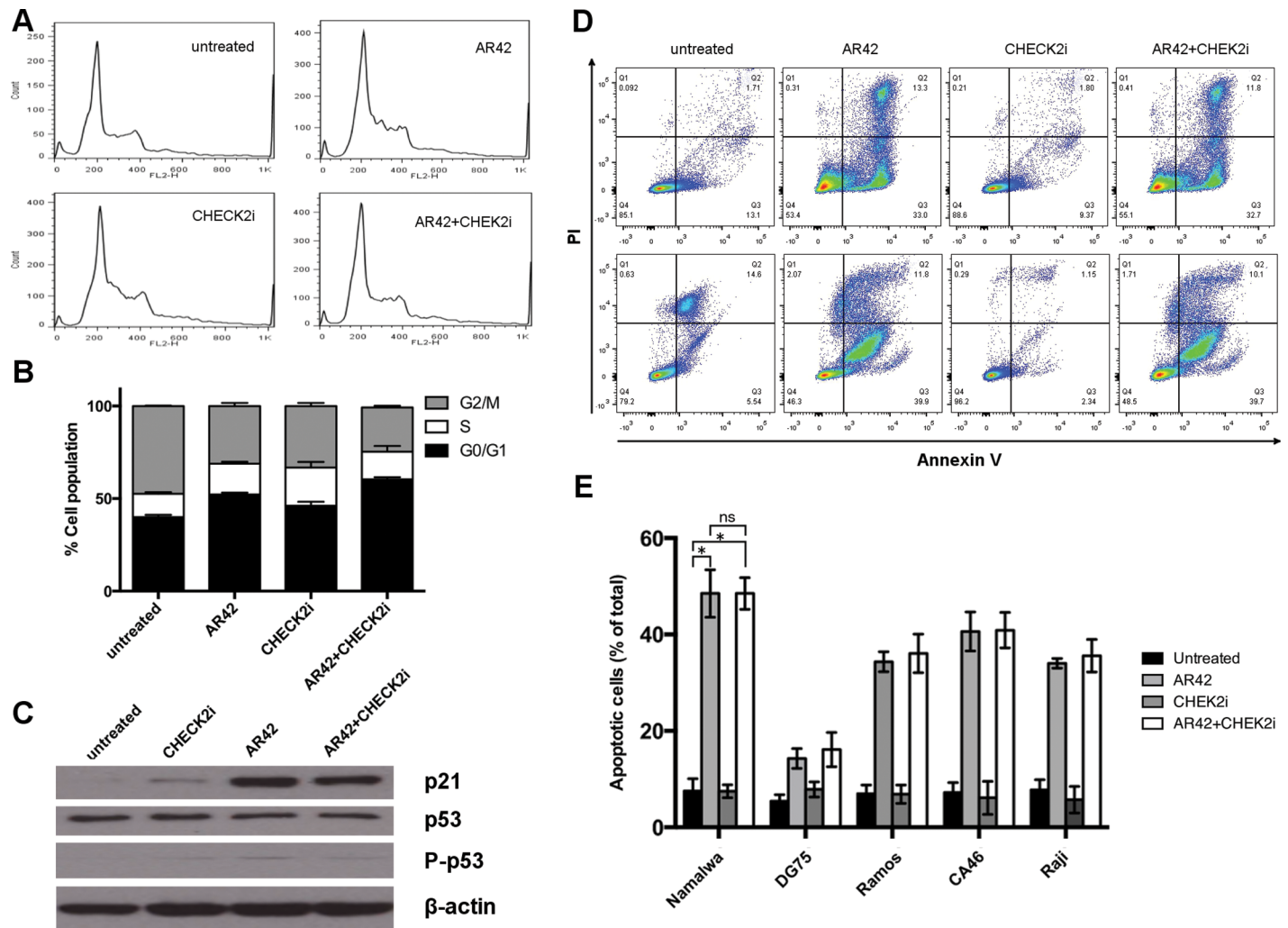


**Figure 2.** CHEK2i and AR42 effect on cell cycle and apoptosis. Raji cells were treated with AR42 (1  $\mu\text{mol/L}$ ), CHEK2i (5  $\mu\text{mol/L}$ ) or both (1  $\mu\text{mol/L}$  AR42 + 5  $\mu\text{mol/L}$  CHEK2i); the cell cycle was assessed by PI staining and apoptosis by annexin V staining. (A) Representative histograms of PI signal by flow cytometry. (B) Quantification of subpopulations at different phases of the cell cycle shows that the combination treatment significantly increased the percentage of cells at the G0/G1 phase, suggesting G1 blockade. Statistical significance of the results is presented in Table 3. (C) Immunoblot analysis indicated p53-independent upregulation of p21 upon AR42 treatment. (D) Representative flow cytometry plots (CA46) for untreated cells and cells treated with either drug alone or in combination for 16 h (top panel) and 72 h (bottom panel). (E) Quantification of the early apoptotic population (Q3 in (D) above). Results are indicated as the mean of three independent experiments where 50,000 events/sample were acquired. Error bars represent standard deviation. Asterisks indicate statistically significantly differences ( $p < 0.01$ ) and are indicated for the first set only for simplicity; statistical significance was the same for all cell lines. ns, Not significant.

**AR42 and CHEK2i Inhibit Growth in Soft Agar**

To further validate the anticancer activity of AR42 and CHEK2i, we examined the ability of these drugs to inhibit *in vitro* anchorage-independent growth of Raji cells (30). AR42 effectively reduced colony formation on soft agar when compared with

untreated controls ( $p = 0.0021$ , Figure 3). Treatment with CHEK2i resulted in a slightly reduced number of colonies, which was not significant ( $p = 0.081$ ). However, treatment with the combination of both inhibitors resulted in more inhibition when compared with either AR42 alone ( $p = 0.008$ ) or CHEK2i alone ( $p = 0.0002$ ), indicating that CHEK2i

potentiated AR42's inhibition of anchorage-independent growth.

**In Vivo Lymphomacidal Activity of AR42 and CHEK2i**

To assess preclinical efficacy and validate the previous *in vitro* findings, nude mice bearing Raji xenografts were used. Cells were implanted in previously

**Table 3.** Tukey multiple comparisons test for the effect of treatments on cell cycle.

	Mean difference	95% CI	Significant?	Summary
G0/G1				
Untreated versus AR42	-12.24	-17.34 to -7.15	Yes	****
Untreated versus CHEK2i	-6.19	-11.28 to -1.01	Yes	**
Untreated versus combination	-20.38	-25.47 to -15.29	Yes	****
AR42 versus CHEK2i	6.06	0.96 to 11.15	Yes	*
AR42 versus combination	-8.18	-13.23 to -3.04	Yes	***
CHEK2i versus combination	-14.19	-19.29 to -9.10	Yes	****
S				
Untreated versus AR42	-4.13	-9.22 to 0.96	No	ns
Untreated versus CHEK2i	-8.07	-13.16 to -2.98	Yes	***
Untreated versus combination	-2.43	-7.52 to 2.66	No	ns
AR42 versus CHEK2i	-3.93	-9.02 to 1.16	No	ns
AR42 versus combination	1.71	-3.38 to 6.80	No	ns
CHEK2i versus combination	5.64	0.55 to 10.73	Yes	*
G2/M				
Untreated versus AR42	16.38	11.28 to 21.47	Yes	****
Untreated versus CHEK2i	14.25	9.16 to 19.35	Yes	****
Untreated versus combination	23.58	18.49 to 28.68	Yes	****
AR42 versus CHEK2i	-2.12	-7.22 to 2.97	No	ns
AR42 versus combination	7.21	2.12 to 12.30	Yes	**
CHEK2i versus combination	9.33	4.24 to 14.42	Yes	****

ns, Not significant; \* $p < 0.05$ ; \*\* $p < 0.01$ ; \*\*\* $p < 0.001$ ; \*\*\*\* $p < 0.0001$ .

irradiated mice and treatment initiated when tumors reached  $>300 \text{ mm}^3$ . When compared with control animals (vehicle alone), CHEK2i dramatically blocked tumor progression (Figure 4A), which is consistent with reports in other cancer models and our own previous findings (14), AR42 also significantly inhibited progression of NHL xenografts in this model. Moreover, the combination of AR42 and CHEK2i was even more effective than either drug alone. Mice treated with either of the inhibitors alone showed relatively stable tumor burden, which did not exceed  $700 \text{ mm}^3$  for the duration of the study. In contrast, mice subject to the combination treatment showed tumor regression after 3 wks of treatment, and this persisted for the duration of the study, with tumors  $< 300 \text{ mm}^3$ . When tumors were dissected at the end of the study, we found that the average tumor weight from untreated animals was  $1.55 \pm 0.89 \text{ g}$

(Figure 4B), while tumors from mice treated with AR42 or CHEK2i were  $0.46 \pm 0.31$  and  $0.49 \pm 0.41 \text{ g}$  respectively, representing a 60% reduction in weight when compared with untreated controls. The average tumor weight from animals treated with the combination of AR42 and CHEK2i was  $0.21 \pm 0.2 \text{ g}$ , representing a reduction of 86% when compared with untreated controls, 54% when compared with AR42 alone and 57% when compared with CHEK2i alone. It should be noted that tumor weight differences for either drug alone versus the combination was not statistically significant in this study; however, duration of the treatment, the kinetics of response and/or initial tumor burden were not assessed and may alter this endpoint.

To assess toxicity of the individual drugs or the combination, body weight was monitored throughout treatment and blood was collected for cell counts and chemistries. No significant body weight

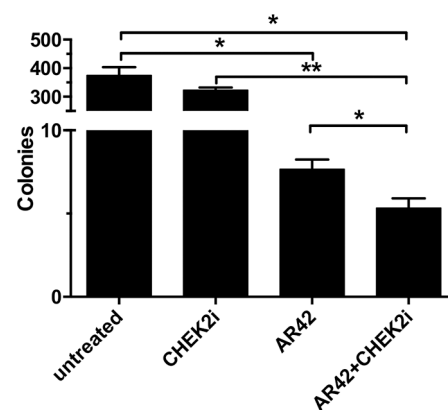


**Figure 3.** CHEK2i and AR42 reduce anchorage-independent growth. Colony formation assays were performed with Raji cells on semisolid medium treated with CHEK2i ( $5 \mu\text{mol/L}$ ), AR42 ( $1 \mu\text{mol/L}$ ), or both. AR42 significantly inhibited colony formation, but the combination treatment was the most effective (\* $p < 0.01$ ; \*\* $p < 0.001$ ).

difference was observed in any of the treatment groups when compared with controls (Figure 5A), blood cells, platelets and hemoglobin remained at normal levels (Figures 5B–E) and both liver (Figures 5F, G) and renal (Figures 5H, I) function were preserved in all treatment groups.

## DISCUSSION

### *In Vitro* Cytotoxicity of AR42 and CHEK2i

AR42 has only recently been evaluated as a cancer therapeutic. It is a pan-HDAC inhibitor and has been shown to suppress tumor growth in U87MG glioblastoma and PC-3 prostate cancer cells by disrupting HDAC-protein phosphatase 1 (PP1) complexes (5). Previous reports have shown that AR42 blocks cancer cell proliferation and elicits cell cycle arrest (4), and it has been reported to be effective against B-cell malignancies by inducing caspase-dependent apoptosis (7,31). Indeed, several HDACs are now in clinical trials for a range of cancers. Checkpoint inhibition represents a more established anticancer therapy (32). CHEK1 and CHEK2 are key components of the DNA-damage response, and

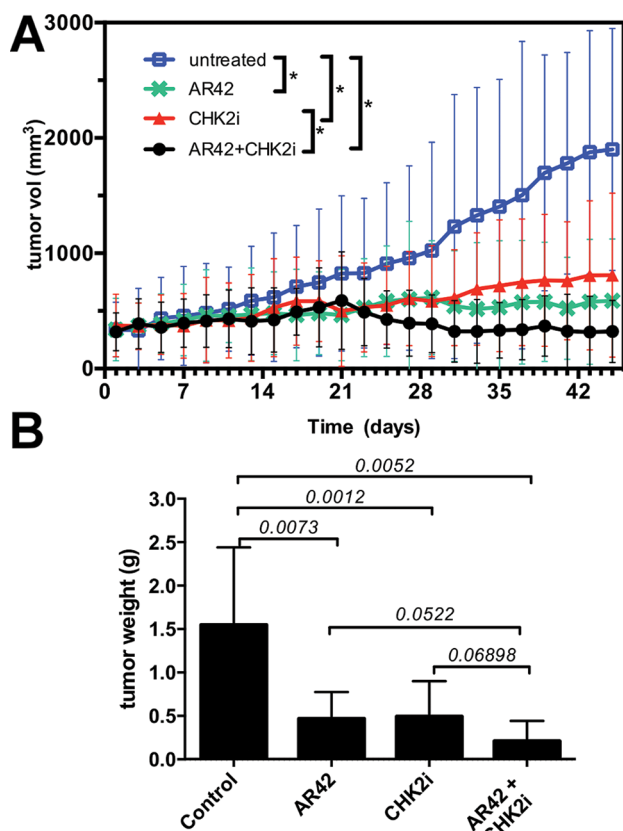


**Figure 4.** *In vivo* efficacy of AR42 and CHEK2i. (A) Tumor volume was assessed in nude mice bearing Raji xenografts treated with AR42, CHEK2i or the combination over 45 d. Control mice tumor-bearing were treated with vehicle only. The combination treatment resulted in the most dramatic tumor growth inhibition. Asterisks indicate statistically significant differences ( $p < 0.05$ , 2-way ANOVA,  $\alpha = 0.05$ , Tukey multiple comparison test) (B) Tumor weight at the end of the study indicated that treatment with CHEK2i or AR42 resulted in significantly smaller tumors; combination treatment resulted in tumors of approximately half the weight ( $n = 7$  mice/treatment; numbers above bars indicate  $p$  values).

inhibitors to these kinases lead to checkpoint abrogation, inhibition of DNA repair and cell death (10,32). Many current cancer treatments are based on DNA damage, and their efficacy is dependent on the cellular response to such damage. Therefore, CHEK inhibitors have been studied extensively in combination with radiation and DNA-damaging drugs, and several have entered clinical trials (33–35). However, not nearly as much research effort has been invested in the study of CHEK inhibition in combination with other cancer therapeutic approaches.

Numerous studies have attempted to use HDACi in combination treatments,

showing both additive and synergistic activity (36). Several reports have shown successful results in multiple myeloma (37–39). Here, we present evidence for the first time that AR42 and CHEK2i show promising preclinical activity using a human NHL xenograft model.

The results presented herein indicate that the combination of AR42 and CHEK2i has higher cytotoxic activity than either drug alone; this is supported by similar results obtained in five NHL cell lines. Individual  $IC_{50}$  values presented in Table 1 closely match  $IC_{50}$ s determined in previous studies from our lab (14) and others (7), further validating our results. In all five cell

lines tested, the combination of both inhibitors resulted in a four- to 10-fold increase in potency, supporting our hypothesis that these agents are more effective when combined.

In an effort to understand the mechanism by which the combination of these agents produce enhanced cytotoxicity, we examined the effects on the cell cycle progression and apoptosis. Not surprisingly, CHEK2i modulated cell cycle progression by enhancing entry of cells into S phase by inhibiting G1 checkpoint. Previous reports have also shown that AR42 blocked cell cycle progression (4). When the two drugs were used together, they produced an additive effect on cell cycle progression, as cells in the G0/G1 phase increased from approximately 40% to almost 60%. The major mechanism of HDACi is believed to be through changes in the transcription of several genes involved in proliferation and cell cycle regulation. In particular, AR42 upregulates expression of p21 (40,41). This protein is known to bind to CDK/cyclin complexes and decrease kinase activation, which leads to cell accumulation in the S and G2/M. On the other hand, several different HDACi have been shown to increase expression of p21 in several different tumor cell lines (42,43). CHEK2 also has been shown to activate p21 (44). In our experiments, we observed a modest induction of p21 upon treatment with CHEK2i and, in agreement with previous reports, a very significant increase in p21 levels when cells were treated with the HDACi AR42. However, the combination of AR42 and CHEK2 inhibition did not further increase p21 above levels seen with each agent alone, which suggests that additional mechanisms that are independent of p21 are responsible for the increase in cytotoxicity and the accumulation in G0/G1. Furthermore, AR42 markedly induced apoptosis as measured by annexin V staining, but CHEK2i did not, and the combination did not enhance the apoptotic effect of AR42. Therefore, the *in vitro* and *in vivo* observations presented in this paper



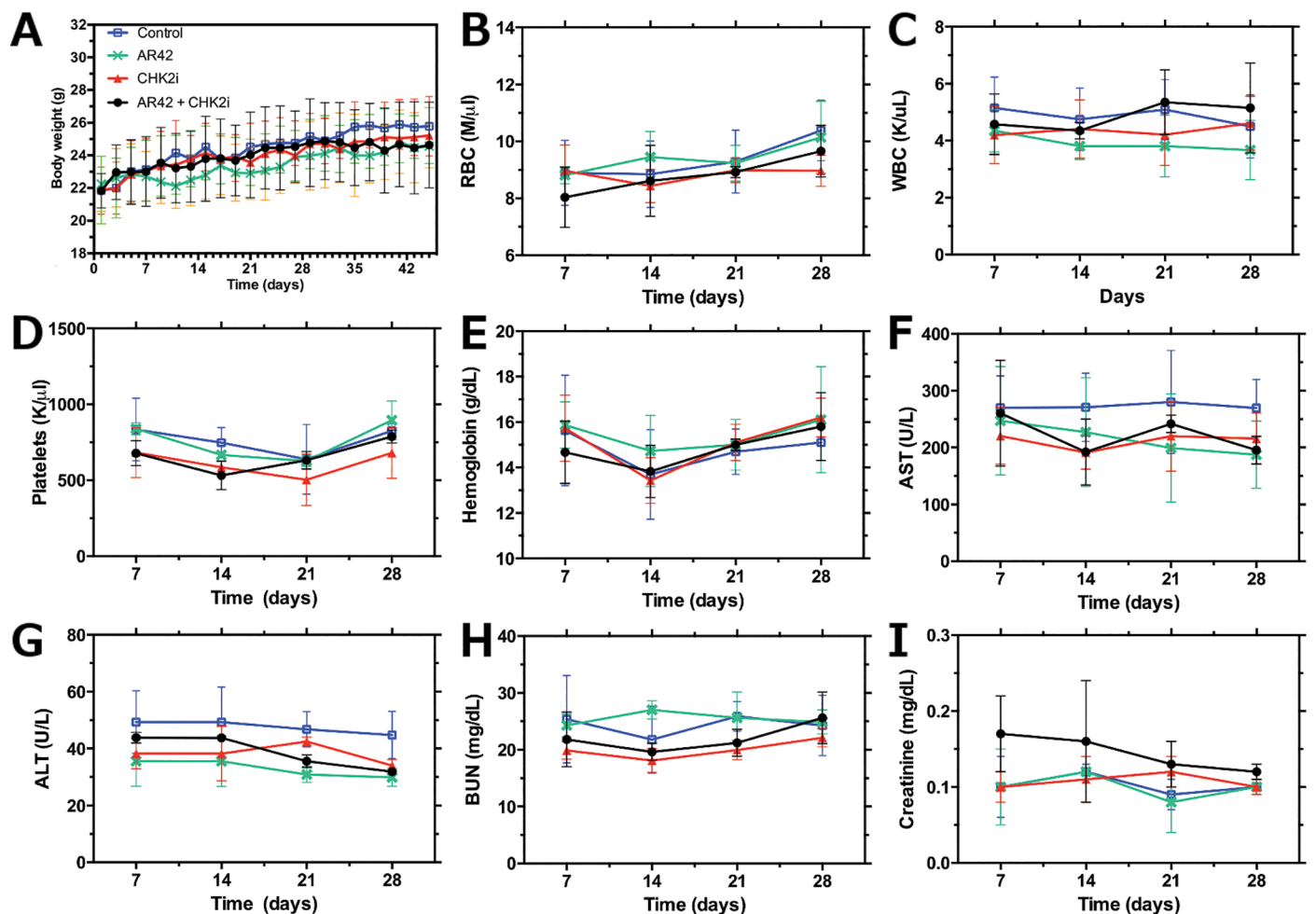


**Figure 5.** Treatment toxicity evaluation. No signs of toxicity were observed in any of the treatment groups as assessed by: body weight (A), hematologic parameters (B–E) and hepatic (F, G) and renal (H, I) function. RBC: red blood cells; WBC: white blood cells; AST: aspartate aminotransferase (plasma); ALT: alanine aminotransferase (plasma); BUN: blood urea nitrogen.

cannot be explained solely by increased activation of the p21 pathway or by the triggering of apoptotic pathways. Clearly, other cellular signaling, cell cycle regulatory and/or apoptotic mechanisms must be at play; understanding of this is the focus of further studies.

Cancer cells are known for their ability to proliferate independently of external signals. Anchorage-independent growth is an acquired characteristic of transformed cells, which can be evaluated *in vitro* by their ability to form colonies in soft agar (30). In this study we evaluated the efficacy of AR42 in combination with CHEK2i in inhibiting anchorage-independent proliferation of Raji cells. Consistent

with *in vitro* cytotoxicity and the *in vivo* antitumor activities described herein, AR42 and, to a lesser extent, CHEK2i effectively inhibited colony formation in soft agar. When used in combination, CHEK2i further enhanced AR42-mediated inhibition. Previous results with different HDACi (vorinostat and panobinostat) showed only temporary colony inhibition in a colorectal cancer cell model (45). The current results suggest that CHEK2 inhibition may be an effective way to improve on the HDACi antitumor properties.

## CONCLUSION

The results described thus far justify evaluation of the combination

treatment in additional *in vivo* human NHL xenograft models that represent the different subtypes of lymphoma seen clinically, and this could set the basis for future clinical evaluation. Using a Raji xenograft model, we present evidence here that the combination of AR42 and CHEK2i improved preclinical efficacy when compared with either drug alone. Furthermore, the combination treatment has no significant toxicity as assessed by body weight, blood counts and blood chemistry. Based on our findings, we propose that HDAC inhibition and CHEK2 inhibition is an attractive combination for further investigation.

## ACKNOWLEDGMENTS

This work was supported by the Schwedler Family Foundation and the deLeuze Non-Toxic Cure for Lymphoma Fund.

## DISCLOSURE

The authors declare they have no competing interests as defined by *Molecular Medicine*, or other interests that might be perceived to influence the results and discussion reported in this paper.

## REFERENCES

- Cheson BD, et al. (2007) Revised response criteria for malignant lymphoma. *J. Clin. Oncol.* 25:579–86.
- Greiner TC, Medeiros LJ, Jaffe ES. (1995) Non-Hodgkin's lymphoma. *Cancer*. 75(1 Suppl):370–80.
- Shankland KR, Armitage JO, Hancock BW. (2012) Non-Hodgkin lymphoma. *Lancet*. 380:848–57.
- Bush ML, et al. (2011) AR42, a novel histone deacetylase inhibitor, as a potential therapy for vestibular schwannomas and meningiomas. *Neuro. Oncol.* 13:983–99.
- Chen CS, et al. (2005) Histone acetylation-independent effect of histone deacetylase inhibitors on Akt through the reshuffling of protein phosphatase 1 complexes. *J. Biol. Chem.* 280:38879–87.
- Jacob A, et al. (2012) Preclinical validation of AR42, a novel histone deacetylase inhibitor, as treatment for vestibular schwannomas. *Laryngoscope*. 122:174–89.
- Lucas DM, et al. (2010) The novel deacetylase inhibitor AR-42 demonstrates pre-clinical activity in B-cell malignancies in vitro and in vivo. *PLoS One*. 5: e10941.
- Balch C, et al. (2012) A unique histone deacetylase inhibitor alters microRNA expression and signal transduction in chemoresistant ovarian cancer cells. *Cancer Biol. Ther.* 13:681–93.
- Sargeant AM, et al. (2008) OSU-HDAC42, a histone deacetylase inhibitor, blocks prostate tumor progression in the transgenic adenocarcinoma of the mouse prostate model. *Cancer Res.* 68:3999–4009.
- Zimmerman B, et al. (2011) Efficacy of novel histone deacetylase inhibitor, AR42, in a mouse model of, human T-lymphotropic virus type 1 adult T cell lymphoma. *Leuk. Res.* 35:1491–7.
- Zhao WL, et al. (2007) Combined effects of histone deacetylase inhibitor and rituximab on non-Hodgkin's B-lymphoma cells apoptosis. *Exp. Hematol.* 35:1801–11.
- Shimizu R, et al. (2010) HDAC inhibitors augment cytotoxic activity of rituximab by upregulating CD20 expression on lymphoma cells. *Leukemia*. 24:1760–8.
- Shi W, et al. (2012) Combined effect of histone deacetylase inhibitor suberoylanilide hydroxamic acid and anti-CD20 monoclonal antibody rituximab on mantle cell lymphoma cells apoptosis. *Leuk. Res.* 36:749–55.
- Kong Y, et al. (2014) Histone deacetylase inhibition enhances the lymphomacidal activity of the anti-CD22 monoclonal antibody HB22.7. *Leuk. Res.* 38:1320–26.
- Xu WS, Parmigiani RB, Marks PA. (2007) Histone deacetylase inhibitors: molecular mechanisms of action. *Oncogene*. 26:5541–52.
- Minucci S, Pelicci PG. (2006) Histone deacetylase inhibitors and the promise of epigenetic (and more) treatments for cancer. *Nat. Rev. Cancer.* 6:38–51.
- Byrd JC, et al. (2005) A phase 1 and pharmacodynamic study of depsipeptide (FK228) in chronic lymphocytic leukemia and acute myeloid leukemia. *Blood*. 105:959–67.
- Sampath D, et al. (2012) Histone deacetylases mediate the silencing of miR-15a, miR-16, and miR-29b in chronic lymphocytic leukemia. *Blood*. 119:1162–72.
- Kulp SK, et al. (2006) Antitumor effects of a novel phenylbutyrate-based histone deacetylase inhibitor, (S)-HDAC-42, in prostate cancer. *Clin. Cancer Res.* 12:5199–206.
- Lu YS, et al. (2007) Efficacy of a novel histone deacetylase inhibitor in murine models of hepatocellular carcinoma. *Hepatology*. 46:1119–30.
- Pommier Y, et al. (2006) Chk2 molecular interaction map and rationale for Chk2 inhibitors. *Clin. Cancer Res.* 12:2657–61.
- Lovly CM, et al. (2008) Regulation of Chk2 ubiquitination and signaling through autophosphorylation of serine 379. *Mol. Cell. Biol.* 28:5874–85.
- Stolz A, et al. (2010) The CHK2-BRCA1 tumour suppressor pathway ensures chromosomal stability in human somatic cells. *Nat. Cell. Biol.* 12:492–9.
- Castedo M, et al. (2004) The cell cycle checkpoint kinase Chk2 is a negative regulator of mitotic catastrophe. *Oncogene*. 23:4353–61.
- Perona R, et al. (2008) Role of CHK2 in cancer development. *Clin. Transl. Oncol.* 10:538–42.
- Ferrao PT, et al. (2012) Efficacy of CHK inhibitors as single agents in MYC-driven lymphoma cells. *Oncogene*. 31:1661–72.
- Dai B, et al. (2011) Functional and molecular interactions between ERK and CHK2 in diffuse large B-cell lymphoma. *Nat. Commun.* 2:402.
- Chou TC, Martin N. (2005) *CompuSyn for Drug Combinations and for General Dose-Effect Analysis*. Paramus (NJ): ComboSyn, Inc. Available from: <http://www.combosyn.com/feature.html>
- Chou TC, Talalay P. (1981) Generalized equations for the analysis of inhibitions of Michaelis-Menten and higher-order kinetic systems with two or more mutually exclusive and nonexclusive inhibitors. *Eur. J. Biochem.* 115:207–16.
- Cifone MA, Fidler IJ. (1980) Correlation of patterns of anchorage-independent growth with in vivo behavior of cells from a murine fibrosarcoma. *Proc. Natl. Acad. Sci. U. S. A.* 77:1039–43.
- Lucas DM, et al. (2004) The histone deacetylase inhibitor MS-275 induces caspase-dependent apoptosis in B-cell chronic lymphocytic leukemia cells. *Leukemia*. 18:1207–14.
- Garrett MD, Collins I. (2011) Anticancer therapy with checkpoint inhibitors: what, where and when? *Trends Pharmacol. Sci.* 32:308–16.
- Ma CX, Janetka JW, Piwnicka-Worms H. (2011) Death by releasing the breaks: CHK1 inhibitors as cancer therapeutics. *Trends Mol. Med.* 17:88–96.
- Dai Y, Grant S. (2010) New insights into checkpoint kinase 1 in the DNA damage response signaling network. *Clin. Cancer Res.* 16:376–83.
- Bucher N, Britten CD. (2008) G2 checkpoint abrogation and checkpoint kinase-1 targeting in the treatment of cancer. *Br. J. Cancer.* 98:523–8.
- Ma X, Ezzeldin HH, Diasio RB. (2009) Histone deacetylase inhibitors: current status and overview of recent clinical trials. *Drugs*. 69:1911–34.
- Wang J, et al. (2013) Potential advantages of CUDC-101, a multitargeted HDAC, EGFR, and HER2 inhibitor, in treating drug resistance and preventing cancer cell migration and invasion. *Mol. Cancer Ther.* 12:925–36.
- Lee CK, et al. (2010) HDAC inhibition synergistically enhances alkylator-induced DNA damage responses and apoptosis in multiple myeloma cells. *Cancer Lett.* 296:233–40.
- Sanchez E, et al. (2011) The histone deacetylase inhibitor LBH589 enhances the anti-myeloma effects of chemotherapy in vitro and in vivo. *Leuk. Res.* 35:373–9.
- Hildmann C, Riester D, Schwienhorst A. (2007) Histone deacetylases—an important class of cellular regulators with a variety of functions. *Appl. Microbiol. Biotechnol.* 75:487–97.
- Lin TY, et al. (2010) AR-42, a novel HDAC inhibitor, exhibits biologic activity against malignant mast cell lines via down-regulation of constitutively activated Kit. *Blood*. 115:4217–25.
- Sasakawa Y, et al. (2003) Effects of FK228, a novel histone deacetylase inhibitor, on tumor growth and expression of p21 and c-myc genes in vivo. *Cancer Lett.* 195:161–8.
- Sasakawa Y, et al. (2002) Effects of FK228, a novel histone deacetylase inhibitor, on human lymphoma U-937 cells in vitro and in vivo. *Biochem. Pharmacol.* 64:1079–90.
- Yun HJ, et al. (2012) Widdrol activates DNA damage checkpoint through the signaling Chk2-p53-Cdc25A-p21-MCM4 pathway in HT29 cells. *Mol. Cell. Biochem.* 363:281–9.
- Wilson PM, et al. (2013) Sustained inhibition of deacetylases is required for the antitumor activity of the histone deacetylase inhibitors panobinostat and vorinostat in models of colorectal cancer. *Invest. New Drugs.* 31:845–57.

Cite this article as: Kong Y, Barisone GA, Sidhu RS, O'Donnell RT, Tusciano JM. (2015) Efficacy of combined histone deacetylase and checkpoint kinase inhibition in a preclinical model of human Burkitt lymphoma. *Mol. Med.* 21:824–32.